

EDDY CURRENT SENSOR CONCEPTS FOR INTERFACE CHARACTERIZATION DURING BRIDGMAN GROWTH OF CdZnTe SINGLE CRYSTALS

Kumar P. Dharmasena and Haydn N.G. Wadley
Intelligent Processing of Materials Laboratory
School of Engineering and Applied Science
University of Virginia
Charlottesville, VA 22903

INTRODUCTION

Hg_{1-x}Cd_xTe Infrared (IR) focal plane arrays are today manufactured on IR transparent CdTe or (lattice matched) Cd_{1-y}Zn_yTe substrates obtained from single crystals grown by a Bridgman method using furnaces with a temperature gradient [1-4]. The yield of single crystal substrate material produced by this method is poor, in part because of the absence of sensor techniques to characterize (and allow control of) the liquid-solid interface shape during crystal growth. This interface, which represents the melting point isotherm of the system, may be convex, ideally flat, or concave. It is determined by heat flow near the interface which is governed, in part, by where solidification occurs in the furnace.

The substrate crystals are grown in furnaces with a steep temperature gradient along the growth axis. When the solid is convex, the sides of the ampoule are above the melting point implying the region must be receiving heat flux from the surrounding furnace. In this case, the interface must be located in the hottest part of the furnace [5]. For the interface to be concave, the sides of the ampoule are below the melting point implying the solidification to be occurring in a cooler region of the furnace. For Cd(Zn)Te, which has a very low solid thermal conductivity, and exhibits supercooling of the liquid, it can be difficult to force solidification to occur at the most desirable position within the temperature gradient of the crystal grower (especially when heat flow is perturbed by ampoule end effects). Thus the optimal interface shape (flat) is quite difficult to achieve and maintain throughout growth. Failure to achieve a flat interface results in large radial thermal stresses (resulting in dislocation generation) and the nucleation of secondary grains at the ampoule wall [6] and has stimulated a need for in-situ interface shape sensors.

There are large differences in the electrical conductivities of solid and liquid CdTe and it is natural to look to the use of eddy current methods to determine the shape and location of the liquid-solid interface during Bridgman growth of Cd(Zn)Te. Since it is costly, time consuming, and imprecise in the absence of independent methods of determining interface shape to equip a crystal grower with eddy current sensors and

experimentally optimize a sensor approach, we are pursuing a modelling approach. The models can also be used to understand the complex eddy current interaction with the electrically inhomogeneous sample and to provide direction to the sensor development path. We report here upon the first results of our approach.

SENSOR CONCEPT

If one considers a volume element enclosing the liquid-solid interface, we expect the eddy current density induced within that element (by a nearby coil) to be strongly affected by the relative fractions of the solid and liquid [7]. Therefore the impedance of an encircling eddy current coil should also be sensitive to these relative fractions. By judicious selection of the excitation frequencies (and therefore the corresponding skin depths of the solid and liquid) it might be possible to infer the interface shape by inversion of multi-frequency eddy current data. For the present, our study is focused only upon indentifying the sensor arrangements which show a maximum sensitivity to changes in interface shape.

SIMULATION MODEL

The eddy current method seeks to exploit the large difference in the solid and liquid phase electrical conductivities of CdTe. Fig.1 shows the variation of electrical conductivity with temperature for CdTe [8]. During the CdTe growth process, the liquid temperature is around 1110°C. For our calculations, we have therefore assumed a constant melt electrical conductivity of 10000 S/m and a constant crystal conductivity of 400 S/m.

Three classes of interface shape (identified by a convexity parameter, θ) were selected for the study. They are shown in Fig.2. They represent the extremes that have been encountered in practice, together with the optimal (flat) shape. Three types of eddy current sensor designs were investigated, Fig.3. They were all of an encircling type,

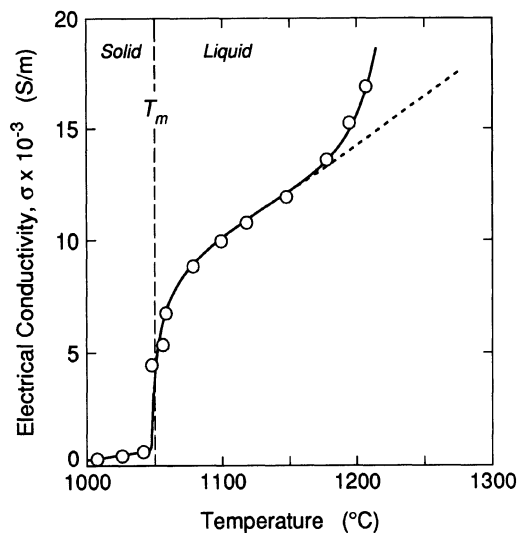


Figure 1. Temperature dependence of electrical conductivity of Cadmium Telluride [8]

utilizing a primary coil and a co-axial secondary coil. The principal differences were the secondary (pick-up) coil arrangements studied. The design of Fig.3(a) had a single secondary coil (referred to as an "absolute" sensor). Those of Figs. 3(b) and 3(c) had two oppositely wound secondary coils to give a differential voltage measurement. They will be referred to as "radially and axially separated differential" sensors respectively.

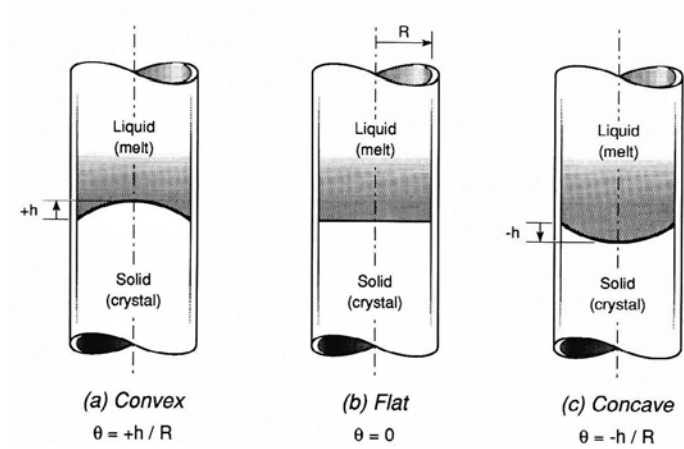


Figure 2. Liquid-Solid Interface shapes chosen for study.

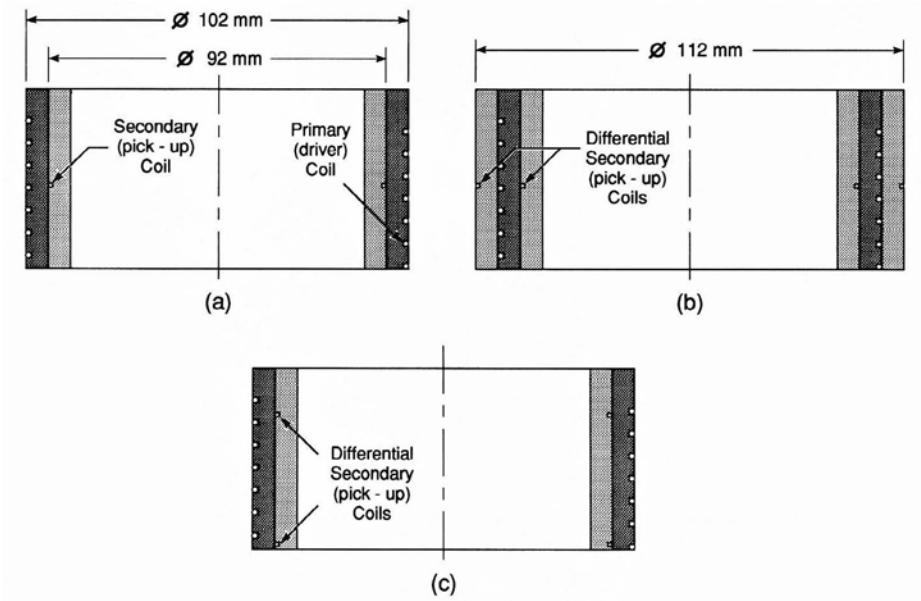


Figure 3. Encircling eddy current sensor designs. (a) Absolute sensor. (b) Radially separated differential sensor. (c) Axially separated differential sensor.

ANALYSIS METHODOLOGY

A commercial electromagnetic finite element analysis package was used for our computations of coil response. We have assumed an axisymmetric model geometry so that only one half of the model needs to be analysed as shown in Fig.4. We have chosen a crystal diameter of 76 mm (3") representative of the largest being attempted by crystal growers. In all, five interfaces, two convex ($\theta = +0.33, +0.66$), one flat ($\theta = 0.$), and two concave ($\theta = -0.33, -0.66$) were modelled. All five interface shapes were incorporated into one model and we used the same finite element mesh for all the analyses. This was accomplished by changing the material properties (i.e. conductivity) of elements near the interface to that of the solid or liquid to represent a different interface condition. Calculations were conducted in the 10kHz-50MHz frequency range. In order to account for the skin effect at high frequencies, the finite element mesh was generated so that smaller elements were used towards the edge of the crystal/melt compared to its center.

The finite element analysis code solves Maxwell's equations for the Magnetic Vector Potential from which physical quantities of interest such as the coil impedance can be calculated. For sinusoidal currents flowing in an axisymmetric "absolute" sensor, Z the coil impedance is given by [7]:

$$Z = \frac{4\pi^2 N_s r_s f}{I_p} [\text{Im}(\underline{A}_{\text{ave}}) - j\text{Re}(\underline{A}_{\text{ave}})] \quad (1)$$

where, N_s is the number of turns of the secondary coil, r_s is the secondary coil radius, f is the frequency and \underline{A}_{ave} is the average vector potential across the cross section of the secondary coil.

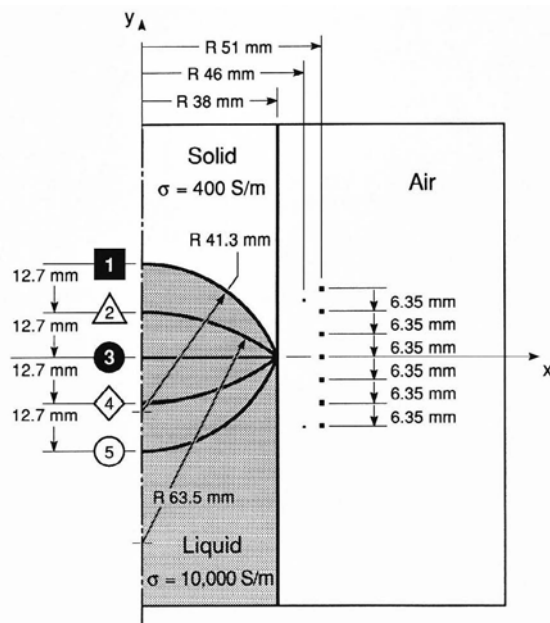


Figure 4. Finite element model geometry.

For two radially separated (i.e. "differential") secondary coils,

$$Z = Z_1 + Z_2 = \frac{4\pi^2 f}{I_p} \left\{ N_{s1} r_{s1} \left[\text{Im}(\underline{A}_{ave}) - j \text{Re}(\underline{A}_{ave}) \right]_1 - N_{s2} r_{s2} \left[\text{Im}(\underline{A}_{ave}) - j \text{Re}(\underline{A}_{ave}) \right]_2 \right\} \quad (2)$$

and for two axially separated differential secondary coils,

$$Z = Z_1 + Z_2 = \frac{4\pi^2 r_s^2 f}{I_p} \left\{ N_{s1} \left[\text{Im}(\underline{A}_{ave}) - j \text{Re}(\underline{A}_{ave}) \right]_1 - N_{s2} \left[\text{Im}(\underline{A}_{ave}) - j \text{Re}(\underline{A}_{ave}) \right]_2 \right\} \quad (3)$$

The calculated impedances are normalized with respect to an empty coil impedance which is found by replacing the "solid" and "liquid" region elements of the model by "air" elements, and repeating the finite element analysis.

RESULTS AND DISCUSSION

Figure 5 shows the normalized reactance (imaginary) component of impedance versus frequency for the single secondary coil (absolute) sensor and three interfaces. At intermediate frequencies (500kHz-1MHz) the impedance shows a clear dependence on the interface shape. As we move outside this frequency range, the dependence on interface shape becomes less prominent and disappears completely at both low and high frequencies. For the intermediate range of frequencies (and skin depths), the fraction of liquid sampled (which is controlled by interface shape) dominates the eddy current sensor's response. At high frequencies, the conductivity at the model's surface controls the response, and this is independent of the interior liquid-solid interface shape. We note that the effects of shape change monotonically, but are relatively small.

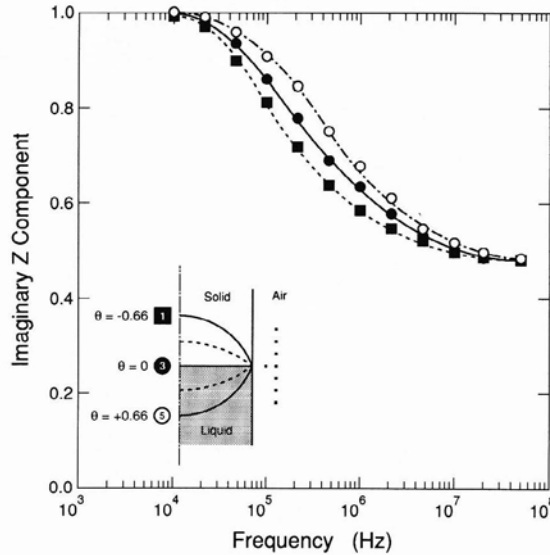


Figure 5. Normalized Reactance component of impedance for the absolute sensor.

Figure 6 shows the case of a radially separated differential coil. Here too the behavior of the impedance curves is similar to that of the absolute coil over the same frequency range. However a comparison of Figs.5 and 6 show that the response of the radially separated differential sensor is more sensitive to interface shape than the absolute coil in the 500kHz-600kHz frequency range.

The normalized reactance component of impedance for the axially separated differential coil and five interfaces is shown in Fig. 7. The axially separated differential sensor shows a greater sensitivity to interface shape than either the absolute sensor or radially separated differential sensors. Again, there is a monotonic trend between sensor response at intermediate frequency and interface convexity, θ (Fig. 8). As in the case of the two previous cases, the ideal frequency range for interface shape determination is between 500kHz and 600kHz.

The differences in reactive impedance response in the 100kHz-1MHz frequency range arises from the differences in electromagnetic flux expulsion from the sample. Because the skin depth in the solid is significantly greater than the liquid, the flux linkage with the sample is sensitive to the liquid-solid interface shape [7]. These differences can be enhanced by the use of a secondary coil design that essentially differentiates the vector potential. The results clearly show that both radial and axial differentiations result in greatly enhanced sensitivity to interface shape.

These calculations have assumed a fixed location of the interface in the sensor. In practice, this location is unknown and is quite likely to vary. We have conducted simulations of this and find that quite small changes in interface height can cause significant changes to the reactive impedance component in the frequency region of interest for interface shape determination. Thus, a change in height could be mistaken for a change in shape and erroneous control actions taken. Further studies show that at very high frequencies ($\sim 50\text{MHz}$) where the liquid and solid skin depths are both small, the impedance

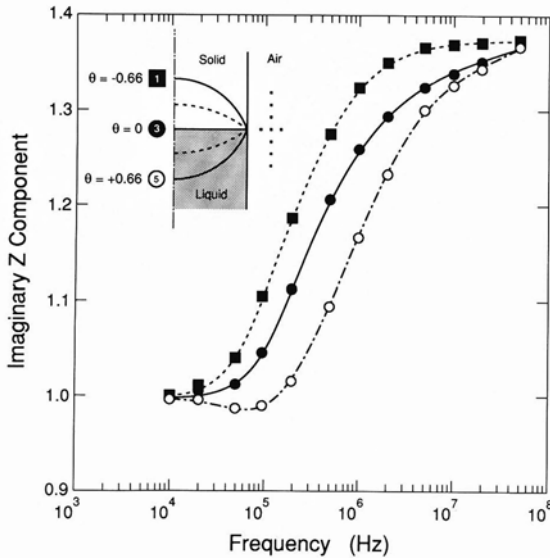


Figure 6. Normalized reactance component of impedance for the radially separated differential sensor.

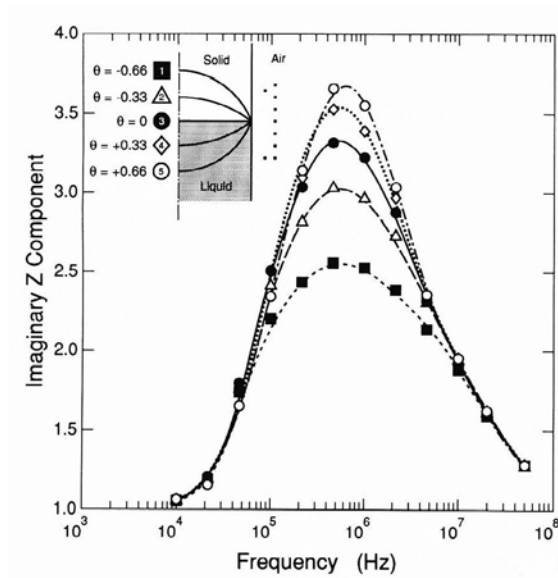


Figure 7. Normalized reactance component of impedance for the axially separated differential sensor.

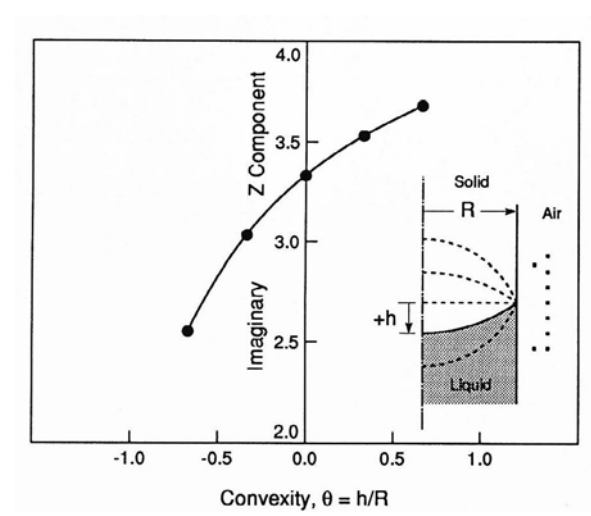


Figure 8. Effect of convexity on the 600kHz normalized reactance impedance component for the axially separated differential sensor

is independent of interface shape depending only upon height. One possible way of deducing the height is to make a second measurement where the effect of height is strong, and to solve simultaneously for the convexity, θ and the position, Δ . Fig.9 shows how the 10MHz reactance impedance component of a radially separated differential sensor varies with position, Δ , of the interface in the sensor. The monotonic variation supports the possibility of using multi-frequency measurements to recover interface shape and melt height.

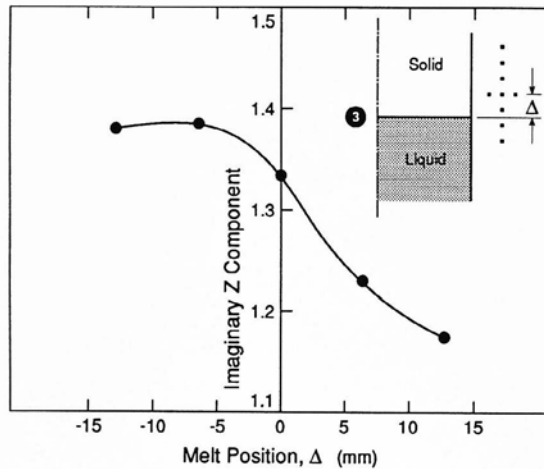


Figure 9. Effect of melt position variation on the 10MHz normalized reactance impedance component for the radially separated differential sensor.

CONCLUSIONS

A need has emerged to measure the shape and location of the liquid-solid interface during Cd(Zn)Te crystal growth. Eddy current methods have been proposed for this because of the large difference in electrical conductivity of the solid and liquid phases. A modelling/simulation approach has been utilized to analyse the design of the sensor and develop methodologies of data analysis. Either radially or axially separated differential sensor designs operating around 600kHz have been found suited for the measurement of interface shape. A radially separated differential sensor or an absolute sensor operating around 5-10MHz shows a strong dependence on melt height and a weaker dependence on interface shape raising the possibility of simultaneous measurement of Δ and θ .

ACKNOWLEDGEMENTS

This work has been conducted as part of the research of the Infrared Materials Producibility Program that includes Johnson Matthey Electronics, Texas Instruments, II-VI Inc., Loral, BDM and the University of Virginia. We are grateful for many helpful discussions with our colleagues in these organizations. This work has been supported by DARPA/CMO under contract MD A972-91-C-0046 monitored by Raymond Balcerak.

REFERENCES

1. M.Pfeiffer and M.Muhlberg, J.Crystal Growth, 118, 269(1992).
2. W.R.Wilcox, F.M.Carlson, D.K.Aidun, V.White, W.Rosch, W.M.Chang, R.Shetty, A.Fritz, R.Balasubramanian, G.Rosen, J.Kweeder and C.Wen, Acta Astronautica, 25, 505(1991).
3. R.Shetty, R.Balasubramanian and W.R.Wilcox, J.Crystal Growth, 100, 51(1990)
4. Handbook on Semiconductors, Vol.4: Device Physics, Ed. C.Hilsum (North-Holland, Amsterdam, 1981).
5. C.E.Chang and W.R.Wilcox, J.Crystal Growth, 21, 135(1974).
6. T.Fu and W.R.Wilcox, J.Crystal Growth, 48, 416(1980).
7. H.N.G.Wadley, K.P.Dharmasena and H.S.Goldberg, in Review of Progress in Quantitative NDE, Vol.10B, 1159(1991).
8. V.M.Glazov, S.N.Chizhevskaya, and N.N.Glagoleva, Liquid Semiconductors, Plenum Press (New York), 1969.